

## RESEARCH ARTICLE

# Age estimation based on 3D pulp segmentation of first molars from CBCT images using U-Net

<sup>1</sup>Yangjing Song, <sup>2</sup>Huifang Yang, <sup>3</sup>Zhipu Ge, <sup>4</sup>Han Du and <sup>1</sup>Gang Li

<sup>1</sup>Department of Oral and Maxillofacial Radiology, Peking University School and Hospital of Stomatology; National Center of Stomatology & National Clinical Research Center for Oral Diseases & National Engineering Laboratory for Digital and Material Technology of Stomatology & Beijing Key Laboratory of Digital Stomatology & Research Center of Engineering and Technology for Computerized Dentistry Ministry of Health & NMPA Key Laboratory for Dental Materials, Beijing, China; <sup>2</sup>Center of Digital Dentistry, Peking University School and Hospital of Stomatology & National Engineering Research Center of Oral Biomaterials and Digital Medical Devices, Beijing, China; <sup>3</sup>Department of Radiology, Qingdao Stomatological Hospital Affiliated to Qingdao University, Qingdao, Shandong Province, China; <sup>4</sup>Shanghai Stomatological Hospital & School of Stomatology, Fudan University & Shanghai Key Laboratory of Craniomaxillofacial Development and Diseases, Fudan University, Shanghai, China

**Objective:** To train a U-Net model to segment the intact pulp cavity of first molars and establish a reliable mathematical model for age estimation.

**Methods:** We trained a U-Net model by 20 sets of cone-beam CT images and this model was able to segment the intact pulp cavity of first molars. Utilizing this model, 239 maxillary first molars and 234 mandibular first molars from 142 males and 135 females aged 15–69 years old were segmented and the intact pulp cavity volumes were calculated, followed by logarithmic regression analysis to establish the mathematical model with age as the dependent variable and pulp cavity volume as the independent variable. Another 256 first molars were collected to estimate ages with the established model. Mean absolute error and root mean square error between the actual and the estimated ages were used to assess the precision and accuracy of the model.

**Results:** The dice similarity coefficient of the U-Net model was 95.6%. The established age estimation model was  $Age = 148.671 - 30.262 \times \ln V$  ( $V$  is the intact pulp cavity volume of the first molars). The coefficient of determination ( $R^2$ ), mean absolute error and root mean square error were 0.662, 6.72 years, and 8.26 years, respectively.

**Conclusion:** The trained U-Net model can accurately segment pulp cavity of the first molars from three-dimensional cone-beam CT images. The segmented pulp cavity volumes could be used to estimate the human ages with reasonable precision and accuracy.

*Dentomaxillofacial Radiology* (2023) **51**, 20230177. doi: [10.1259/dmfr.20230177](https://doi.org/10.1259/dmfr.20230177)

**Cite this article as:** Song Y, Yang H, Ge Z, Du H, Li G. Age estimation based on 3D pulp segmentation of first molars from CBCT images using U-Net. *Dentomaxillofac Radiol* (2023) 10.1259/dmfr.20230177.

**Keywords:** Age estimation; CBCT; First molar; Medical image segmentation; U-Net

## Introduction

Age is a crucial feature in the biological profile reconstruction and personal identification in forensic sciences.<sup>1,2</sup> Teeth are among the most reliable tools in the process of identification because dental tissue is

the hardest and the most durable part of the human body resistant to destruction when one encounters mass disaster or natural calamity, especially the burned, decomposed and severely traumatized case.<sup>3</sup> Another reason that supports teeth provide the most reliable guide to age estimation is age-related change of the pulp volume. After the tooth root is fully developed, secondary dentin deposits on the inner side of the pulp

Correspondence to: Dr Gang Li, E-mail: [kqgang@bjmu.edu.cn](mailto:kqgang@bjmu.edu.cn)

Received 18 April 2023; revised 17 May 2023; accepted 02 June 2023; published online 22 June 2023

**Table 1** Smith and Knight tooth wear index

Score	Tooth surface	Criteria
0	B/L/O/I	No loss of enamel surface characteristics
	C	No loss of contour
1	B/L/O/I	Loss of enamel surface characteristics
	C	Minimal loss of contour
2	B/L/O/	Loss of enamel exposing dentine for less than one third of surface
	I	Loss of enamel just exposing dentine
	C	Defect less than 1 mm deep
3	B/L/O/	Loss of enamel exposing dentine for more than one third of surface
	I	Loss of enamel and substantial loss of dentine
	C	Defect less than 1–2 mm deep
4	B/L/O/	Complete enamel loss-pulp exposure-secondary dentine exposure
	I	Pulp exposure or exposure of secondary dentine
	C	Defect more than 2 mm deep-pulp exposure of secondary dentine exposure

wall with age. This process is lifelong and causes a reduction of pulp cavity.<sup>4</sup> Therefore, indicators related to pulp cavity are considered as a predictor for age estimation.

Dental radiographical examination, which complements the visual examination of dental tissue, is a non-destructive and cost-efficient method and appropriate to be utilized for age estimation,<sup>5</sup> when comparing to time-consuming and destructive histological or biochemical methods which requires sophisticated laboratory equipment and tooth extraction. In 1961, Philippas firstly studied the correlation between secondary dentin and chromosomal age by periapical radiograph.<sup>6</sup> Thereafter, the coronal pulp cavity index was introduced by Ikeda et al in 1985<sup>7</sup> and has been used for age estimation till now.<sup>8–10</sup> Some other parameters of dental tissues such as pulp/tooth length ratio and pulp/tooth area ratio were calculated for age estimation by using two-dimensional images such as panoramic radiograph and periapical radiograph.<sup>11,12</sup> However, secondary dentin formation is a morphologic change in three dimensions that cannot easily be captured through conventional two-dimensional X-ray imaging. With the advent of cone-beam computed tomography (CBCT) and the optimization of image analysis software, researchers began to choose three-dimensional (3D) images for age estimation. Andrade et al extracted the pulp cavity volume of central incisors and canines from CBCT images to certify the correlation between age and pulp cavity volume.<sup>13</sup> The monoradicular teeth such as incisors, canines and maxillary second premolars were also used for age estimation by Kazmi et al, Yang et al and in some other studies.<sup>14–16</sup> However, studies on multiradicular teeth such as the first molar are rare because of the complexity and diversity of the root canal system.

The first molar is the earliest permanent tooth to erupt and should be a suitable for age estimation in forensic odontology. In 2015, Ge et al firstly calculated pulp chamber volumes of first molars using a 3D image semi-automatic segmenting and voxel-counting software ITK-SNAP and established a method used for human age estimation.<sup>17</sup> Further, Zheng et al developed an automatic segmentation method by integrating deep learning and level set to segment the pulp chamber of first molars from CBCT images and estimated ages by calculating pulp chamber volumes.<sup>18</sup> These studies were only limited to the volume of pulp chamber, not the volume of the intact pulp cavity containing pulp chamber and root canals, which may degrade the estimation accuracy. In other words, it has not been conclusively clarified whether the volume of the root pulp yields any additional benefit for the accuracy of age estimation.

With convolutional neural networks outperforming the state of the art in many visual recognition tasks, deep convolutional neural networks, level set and other advanced artificial intelligence are applied in stomatology.<sup>19–23</sup> Among them, U-Net architecture achieves very good performance on different biomedical segmentation applications through very few images relying on an elastic deformation-based data augmentation strategy.<sup>24–26</sup> Some precedents have used U-Net to segment tooth and pulp tissue and demonstrated that it can fast and accurately extract pulp.<sup>26,27</sup>

Above all, the overall aim of this study was to develop a mathematical model for age estimation with the intact pulp cavity volume of first molars segmented by U-Net and to investigate if the model is accurate enough to estimate human age. The hypothesis was that the established model was good enough for the estimation of human age.

## Materials and method

### Training data acquisition

In this study, 20 sets of CBCT image data were collected for U-Net training from the database of Peking University School and Hospital of Stomatology. All the CBCT images were acquired using NewTom VG (Quantitative Radiology, Verona, Italy) and reconstructed with a voxel size of 0.15 mm. The image acquisition parameters were: tube voltage 110 kVp, tube current 2–16 mAs, the field of views (FOVs) 6×6 cm, 8×8 cm, 12×8 cm or 15×15 cm in accordance with patient figure and clinical needs. After being reconstructed with a voxel size of 0.15 mm, the acquired images were exported as DICOM data sets.

The inclusion criteria of first molars were: no caries, no dental restorations, no artifacts due to metal restorative materials present in adjacent teeth or orthodontic appliances, no pulp calcification, no taurodontism, no anomaly, no excessive tooth wear and no severe periodontal disease. To specify the extent of “excessive tooth

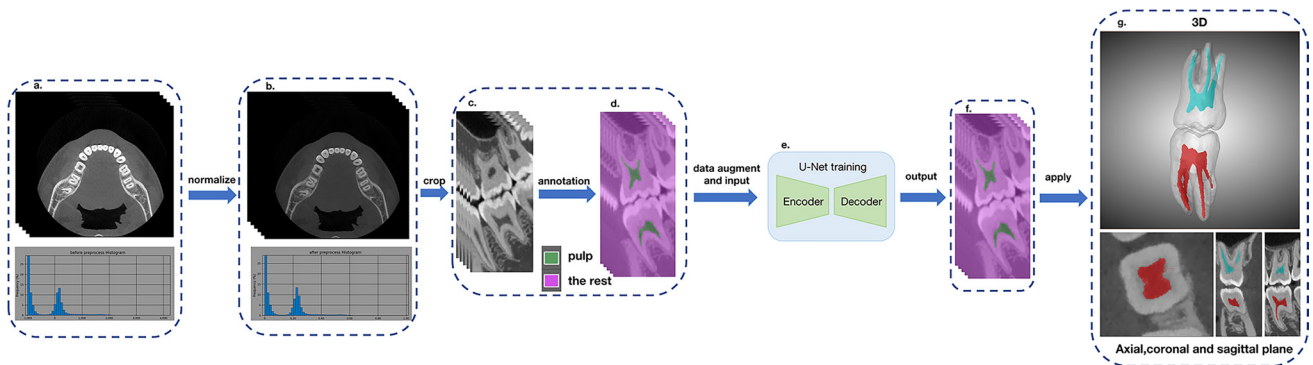


**Figure 1** The work flow of U-net training and pulp cavity segmentation. (a) The original DICOM data sets was imported into Dragonfly. (b) The voxel color gradient of CBCT images were normalized into [0, 1]. (c) The region of interest was cropped into nearly a smallest region only containing the complete first molar. (d) Slices of every CBCT data set from the sagittal plane as input frames and manually annotate pulp and the rest of tooth tissue as two different classes in every frame. (e) The annotated images were performed by data augmentation and input into the U-Net for encoding (downsampling) and decoding (upsampling) to accomplish training. (f) The trained U-Net output segmented images. (g) An example of the segmentation result.

wear”, we borrowed the Smith and Knight’s tooth wear index (TWI, [Table 1](#))<sup>28</sup> and the results from the tooth wear epidemiological investigation in Chinese population.<sup>29</sup> The tooth with TWI ≤2 before 50 years and TWI ≤3 after 50 years was included. To specify the extent of “severe periodontal disease”, we borrowed the new classification of periodontitis in 2018.<sup>30</sup> A tooth with stage ≤3 was included.

*Preprocessing and annotation*

The CBCT image DICOM data sets was imported into an image processing and 3D reconstruction software Dragonfly (v. 2021.1.0.977, Objects Research Systems, Montreal, Canada) for pre-processing and annotation.

To reduce the amount of calculated data, the voxel gray gradient of CBCT images were normalized into [0, 1] through linear transformation. The probability distribution map of the voxel color gradient is shown in [Figure 1\(a and b\)](#). Since this study focused on the segmentation of pulp cavity of first molars, the region of interest was cropped into nearly a smallest region only containing the complete first molar, as shown in [Figure 1\(c\)](#).

To acquire gold-standard labels, every slice of these 20 CBCT data sets was manually annotated into two different classes, pulp and the rest of tooth tissue, as shown in [Figure 1\(d\)](#). Manual annotation was finished by an oral and maxillofacial radiologist.

*Data augmentation*

All frames were performed with data augmentation. Data were augmented 10 times, including flipping horizontally and vertically, rotating maximum 20 degrees, shearing maximum 2 degrees, scaling 90–110% and brightness 0.10–2. Therefore, the quantity of annotated slices increased 10-fold (10,480 in total). Then, 80% of these data was used as the training data set to train the U-Net model, and the rest 20% was used for validation to determine the optimal model.

*U-Net architecture*

In this study, we employed a U-Net network that was embedded in Dragonfly. A schematic overview of the U-Net network is presented in [Figure 2](#). This network is a symmetrical architecture with a contracting path (the right part) to capture context and an expanding path (the left part) that enables precise localization. As the typical architecture of a convolutional network, the contracting path consists of the repeated application of two 3 × 3 convolutions (unpadded convolutions), each followed by a 2 × 2 max pooling operation for downsampling. At each downsampling step, the number of feature channels was doubled. Every step in the expansive path consists of an upsampling of the feature map followed by a 2 × 2 convolution (up-convolution) that halves the number of feature channels, a concatenation with the correspondingly cropped feature map from the contracting path, and two 3 × 3 convolutions, each followed by a rectified linear unit. At the final layer, a 1 × 1 convolution is used to map feature vectors to the desired number of classes.

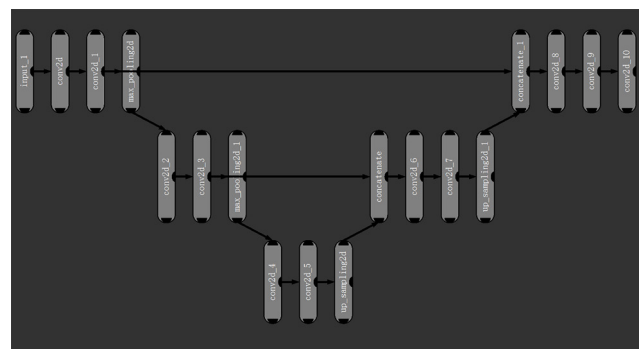


**Figure 2** A schematic overview of the U-Net network.

**Table 2** The number of males and females, maxillary and mandibular first molars, the mandibular first molars with a distolingual root in each age group from the modeling group

Age (year)	Males	Females	Maxillary first molars	Mandibular first molars	Mandibular first molars with a DL root	Right first molars	Left first molars
15–20	19	21	37	38	7	42	33
21–30	30	29	55	52	17	60	47
31–40	29	27	53	50	17	63	40
41–50	27	27	48	43	14	39	52
51–60	25	17	26	30	8	27	29
61–69	12	14	20	21	4	18	23
Total	142	135	239	234	67	249	224

DL, distolingual.

### U-Net training

The training is conducted with 100 epochs, however, it stops if there is no improvement in “value loss” for 10 consecutive epochs. Training parameters were: patch size = (64, 64, 1), stride ratio = 0.25, batch size = 256. For more detailed information, please refer to the previous study.<sup>31</sup>

In dragonfly, dice Loss function ( $L_{dice}$ ) was used to evaluate the performance of the trained U-Net.

$$L_{dice} = -\frac{2\sum_x g_l(x) \log(p_l(x))}{\sum_x g_l(x)^2 + \sum_x p_l(x)^2}$$

where  $p_l(x)$  was the estimated probability of voxel  $x$  belonging to class  $l$ , and  $g_l(x)$  was the manually labeled segmentation masks.

Furthermore, to investigate the difference between the automatic segmentation and manual segmentation, another 40 samples aged from 15 to 69 years old complying with the aforementioned inclusion criteria were randomly selected and segmented by the trained U-Net and two examiners who were familiar with anatomy and had been taught how to use the software. After a 2-week interval, one of the examiners segmented the pulp cavity again.

### Mathematical model establishment

The study was approved by the Institutional Review Board, and the requirement for written informed consent was waived. We retrospectively collected CBCT images from the database of Peking University School and Hospital of Stomatology.

CBCT images of 239 maxillary first molars and 234 mandibular first molars from 142 males and 135 females aged 15–69 years old were included according to the inclusion criteria and regarded as the modeling group. All molars were divided into six groups according to age. The distribution of males and females, left side and right side, maxillary and mandibular first molars and the mandibular first molars with a distolingual (DL) root in each age group are shown in Table 2.

All these CBCT images were obtained with the CBCT unit NewTom VG (Quantitative Radiology, Verona, Italy) and reconstructed with a voxel size of

0.15 mm. All these images were from the Chinese population and the image acquisition parameters were: tube voltage 110 kVp, tube current 4.19–125.32 mAs, FOVs 6×6 cm, 8×8 cm, 12×8 cm or 15×15 cm in accordance with patient figure and clinical needs. After being reconstructed with a voxel size of 0.15 mm, the acquired images were exported as DICOM data sets.

Then, apply the trained U-Net and export the intact pulp volume ( $\text{mm}^3$ ) of all samples based on that volume equals the voxel value multiplied by the number of voxels.

Logarithmic regression analysis was performed by IBM SPSS Statistics 26.0.0.0 (SPSS, IBM, Chicago, IL) with the volume calculated from the pulp cavity segmentation model as a predictor and age as the dependent variable to establish a mathematical model for age estimation.

### Method validation

Another CBCT images of 128 maxillary first molars and 128 mandibular first molars from 42 females and 54 males aged 15–69 years old were collected from the database of Peking University School and Hospital of Stomatology with the same criteria. All samples were also from the Chinese population and regarded as the validation group to calculate the precision and accuracy of the mathematical model. The distribution of males and females, left side and right side, maxillary and mandibular first molars and the mandibular first molars with a distolingual root in each age group are shown in Table 3.

After the procedure of segmentation, the volumes of these samples were obtained. Taking the numerical value of first molars in the validation group into the mathematical model, we obtained these samples' estimated age.

### Statistical analysis

Intraclass correlation coefficients (ICCs) was used to evaluate the manual segmentation agreements within (intra-) and between (inter-) observers. ICC values and their 95% confidence intervals were calculated based on the guideline.<sup>32</sup> The ICC values were interpreted as

**Table 3** The number of males and females, maxillary and mandibular first molars and the mandibular first molars with a distolingual root in each age group from the validation group

Age (year)	Males	Females	Maxillary first molars	Mandibular first molars	Mandibular first molars with a DL root	Right first molars	Left first molars
15–20	8	5	20	21	4	10	15
21–30	12	13	42	38	9	22	25
31–40	14	14	35	32	13	19	33
41–50	10	4	18	17	8	13	14
51–60	6	3	5	9	5	2	4
61–69	4	3	8	11	1	6	8
Total	54	42	128	128	40	72	99

DL, distolingual.

poor (<0.50), moderate (0.50–0.75), good (0.75–0.90), or excellent (>0.90) in agreement.

To investigate the volume difference between the automatic and manual segmentation, paired *t*-test was performed on the 40 samples. A *p*-value of 0.05 or less was considered significantly different. In addition, Bland–Altman analysis was also used for the evaluation of the volume difference.

To investigate whether gender, tooth location (location in the maxilla or mandible, location on the right or left side) and the development with or without a distolingual root have an impact on the accuracy of age estimation, multivariate analysis of variance (MANOVA) was performed for the modeling group. The factor has an impact on the volume of pulp cavity when *p* < 0.05.

Mean absolute error (MAE) and root mean square error (RMSE) between the actual age and estimated age were used to validate the precision and accuracy of the established age estimation model.

## Results

The dice loss function revealed that dice similarity coefficient (DSC) of the trained U-Net model was 95.6%. Automatic segmentation took only 13–33 s while manual segmentation needs 15–25 min. This demonstrates that automatic segmentation is much faster than manual segmentation.

The ICC value for the intraobserver agreement was consistently high (ICC = 0.992), so was the ICC for interobservers (ICC = 0.944). The paired *t*-test demonstrated that there was no significant difference between the manually and automatically segmented volumes (*p* = 0.214). The Bland–Altman analysis indicates the volume differences between the automatic and manual segmentations of the pulp cavities (Figure 3). 37 out of 40 points were within the 95% limits of agreement. Thus, automatic segmentation is accurate and feasible in practical application.

The pulp cavity volumes of first molars in the modeling group ranged from 10.89 to 90.48 mm<sup>3</sup> with the mean value = 43.09 mm<sup>3</sup> and the standard deviation = 16.03 mm<sup>3</sup>. The distribution of volumes in each age group of model establishment and model validation is shown in Figure 4.

The scatter diagram of logarithmic regression analysis for all first molars in the model establishment group shows the relationship between the pulp volumes and ages in Figure 5.

Age estimation mathematical models by logarithmic regression analysis for the modeling group was

$$\text{Age} = 148.671 - 30.262 \times \ln V$$

*V* was the pulp cavity volume.

Plots of actual ages vs estimated ages calculated by the above mathematical model in the validation group are shown in Figure 6. The scatter is evenly distributed on both sides of the diagonal line, which demonstrated that calculation errors had an even distribution.

There was no significant difference for gender (*p* = 0.773), location in the maxilla or mandible (*p* = 0.286), location on the right side or left side (*p* = 0.209) and mandibular first molar with or without a distolingual root (*p* = 0.131).

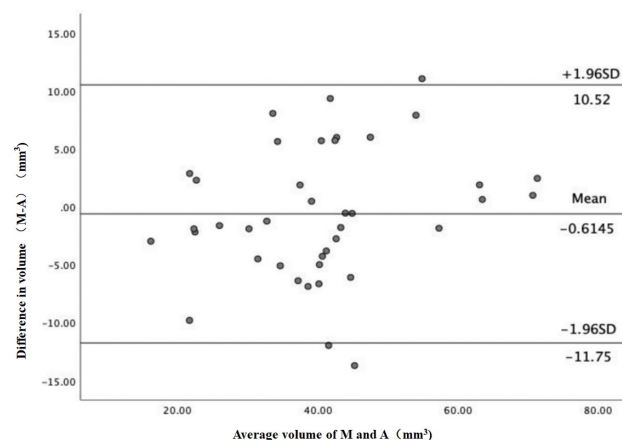


**Figure 3** Differences of pulp cavity volumes obtained from automatic and manual segmentation against mean pulp cavity volumes obtained from automatic and manual segmentation. A, automatic segmentation; M, manual segmentation; SD, standard deviation.

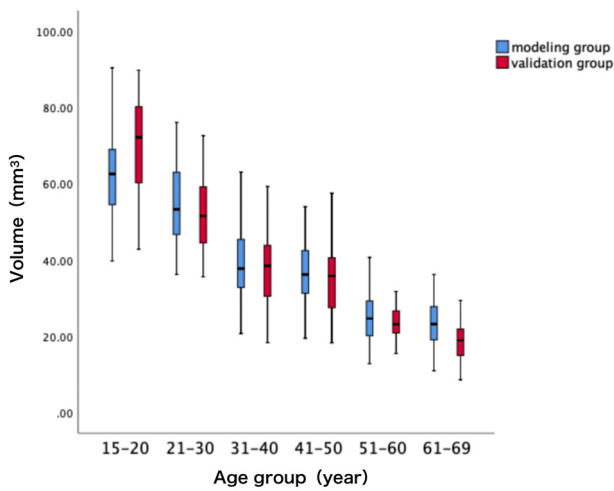


**Figure 4** The distribution of volumes in each age group of the modeling group and the validation group.

MAE and RMSE for all molars in each age group are shown in [Table 4](#).

## Discussion

This study demonstrates that pulp cavity volume from the first molar can be used for age estimation and gives a relatively high correlation between estimated and actual ages ( $R^2 = 0.662$ ) when comparing with the sole use of pulp chamber volumes.<sup>17,18</sup> This result indirectly indicates that the trained U-net model is accurate enough for the segmentation of pulp cavity.

Compared with studies by Ge *et al* and Zheng *et al* in which only pulp chamber volume was employed,<sup>17,18</sup>

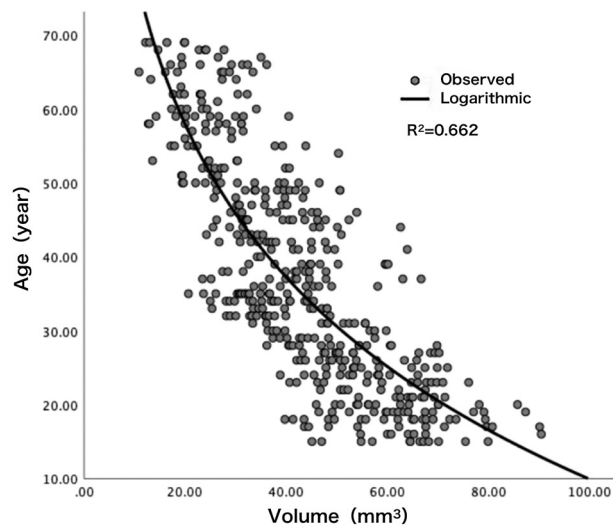


**Figure 5** The scatter diagram of logarithmic regression analysis for the modeling group shows the relationship between pulp volumes and ages.

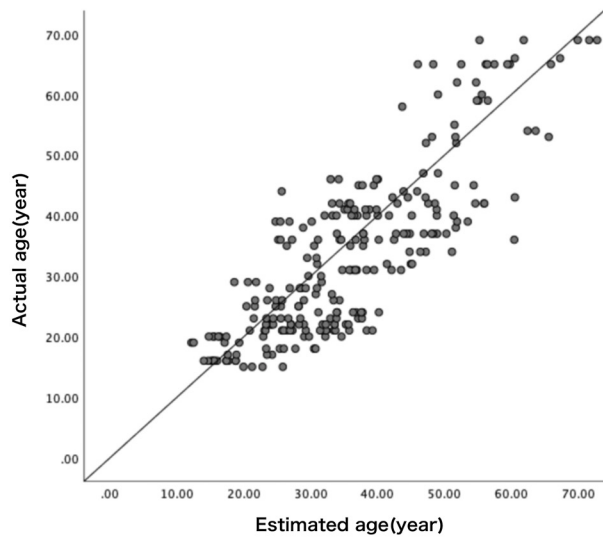


**Figure 6** Plots of actual age versus estimated age for the validation group.

this study employed the full volume of pulp cavity containing not only the pulp chamber but also the root canals. The root canals in molars are difficult to segment manually due to the diversity of root canal morphology, calcification of root canals in old people and software inefficiency. These make manual segmentation of molar root canal time-consuming and inaccurate. It is worth noting that the subjects used for model establishment in the present study were the same as those used in the study by Ge *et al*. Thus, the results from these two studies can be used for direct comparison and the results are favorable for the age estimation model from a full volume of the pulp cavity.

Gender and tooth location may play a role in age estimation by using teeth, which was confirmed by the previous studies from the same samples used in the study.<sup>17</sup> However, after analysis of MANOVA, the difference between genders or tooth locations (right and left side, mandible and maxilla) was not statistically significant. In addition, the existence of a distolingual root for the mandibular molar didn't influence age estimation in spite that the prevalence of the distolingual root is 26.98% ~ 33.75% in Chinese population.<sup>33,34</sup> This finding

**Table 4** MAE and RMSE for each age group from the validation group

Age group (year)	MAE (year)	RMSE (year)
15–20	5.01	6.37
21–30	6.71	8.30
31–40	7.57	8.97
41–50	6.64	8.15
51–60	6.12	7.40
61–69	8.14	9.78
All teeth	6.72	8.26

MAE, mean absolute error; RMSE, root mean square error.

greatly improves the simplicity of practical application. Based on this finding, age can be estimated just using a universal mathematical model especially when gender, tooth location and the development of the distolingual root are unknown. In fact, the remains of the unknown deceased individuals are usually fragmentary, and gender and even tooth positions could not be attested.

Due to the complexity of root canal system in multi-radicular teeth, many studies focused on monoradicular tooth or only the pulp chamber of molars.<sup>13–16</sup> Among the multiple studies involving monoradicular teeth, canine was found to be the least correlated (Kazmi *et al.*  $R^2 = 0.33$  for canine, Haghanifar *et al.*  $R^2=0.392$  for maxillary canine, Molina *et al.*  $R^2 = 0.010$ ).<sup>2,14,35</sup> This may be attributed to the fact that canines are only responsible for tearing food, not for grinding, so the age-related change of pulp cavity volume is small. Incisors have a relatively high correlation (Molina *et al.*  $R^2 = 0.167–0.366$  for upper and lower incisors, Asif *et al.*  $R^2=0.78$  for maxillary central incisors).<sup>2,36</sup> Ge *et al* compared 13 types of teeth including all maxillary and mandibular monoradicular teeth and the first and second molars. They found that the correlation of monoradicular teeth was lower than that of molars ( $R^2 = 0.108–0.344$  for all monoradicular teeth,  $R^2 = 0.434–0.498$  for molars).<sup>37</sup> The  $R^2$  obtained in this study was also higher than that of the aforementioned monoradicular teeth, so we believe that the estimated age using multiradicular teeth is higher than that of monoradicular teeth.

Pulp-to-tooth ratio (PTR) has been assessed frequently in the previous studies for age estimation.<sup>2,15,36</sup> The correlation between PTR and chronological age, however, varies considerably with a  $R^2$  from 0.108 to 0.70.<sup>38</sup> This indicates that PTR is not good enough for dental age estimation and may attributes bias from different types of tooth used. The present study gives a  $R^2$  of 0.662 and if considering the  $R^2$  of 0.564<sup>17</sup> and  $R^2$  of 0.52<sup>39</sup> from the previous studies in which volume of molar pulp chamber is used for age estimation, the volume of molar pulp cavity may be a remarkable index for age estimation. The reason may be in follows. First, the age-related formation of secondary dentine is directly related to the decrease of pulp cavity volume while the volume of an entire tooth is mainly affected by the attrition of enamel, which may be closely related to eating habit. Thus, PTR may not reflect the real change from secondary dentin apposition. Second, the pulp volume calculation is more accurately segmented than the whole tooth volume due to high image contrast between dentin and pulp, low image contrast between enamel and tooth socket.<sup>40</sup>

To evaluate the segmentation result of the trained U-Net, two metrics were used. The first one is DSC, a widely used metric and loss function for biomedical image segmentation due to its robustness to class imbalance and demonstrates good performance of the trained

U-Net. However, DSC has the shortcoming of overconfident prediction that cannot be usefully interpreted in clinical practice.<sup>41</sup> Therefore, paired *t*-test and Bland–Altman analysis were introduced as the second metric. By comparing the volumes of another 40 samples between the manual and automatic segmentations, the reliability of the trained U-Net to segment the pulp was further confirmed.

There are limitations to this study. First, only first molars were included but they are more likely to abrade and lost with age. Consequently, premolars and anterior teeth should also be taken into account to increase the accuracy of age estimation. Secondly, when checking segmentation results, the investigators found that segmentation was coarse in old age groups. So, more state-of-the-art net architectures such as Swin Transformer<sup>42</sup> and DeepLab<sup>43</sup> and imaging post-processing techniques may be helpful to obtain an optimal segmentation model without further manual correction.

## Conclusion

This U-Net can be used to accurately segment the intact pulp cavity of first molars. The intact pulp cavity of multiradicular first molars is a good index for human age estimation with reasonable precision and accuracy without considering factors such as gender, tooth location and the distolingual root.

## Funding

The study was supported by the PKU-Baidu Fund (No. 2020BD037) and the National Key Research and development Program of China (No. 2018YFC0807303).

## Patient consent

Written informed consent was not required for this study because all the included patients in the present investigation were collected retrospectively. Exemption of informed consent will not affect the rights and health of the included patients. The application for free informed consent was approved by the Institutional Review Board.

## Ethics approval

All procedures performed in the study involving human participants were in accordance with the ethical standards of the Institutional Review Board and with the 1964 Helsinki declaration and its later amendments or comparable ethical standards.

## REFERENCES

- Adserias-Garriga J, Thomas C, Ubelaker DH, C Zapico S. When Forensic Odontology met Biochemistry: Multidisciplinary approach in Forensic human identification. *Arch Oral Biol* 2018; **87**: 7–14. <https://doi.org/10.1016/j.archoralbio.2017.12.001>
- Molina A, Bravo M, Fonseca GM, Márquez-Grant N, Martín-de-Las-Heras S. Dental age estimation based on pulp Chamber/crown volume ratio measured on CBCT images in a Spanish population. *Int J Legal Med* 2021; **135**: 359–64. <https://doi.org/10.1007/s00414-020-02377-y>
- Shah P, Velani PR, Lakade L, Dukle S. Teeth in Forensics: A review. *Indian J Dent Res* 2019; **30**: 291–99. [https://doi.org/10.4103/ijdr.IJDR\\_9\\_17](https://doi.org/10.4103/ijdr.IJDR_9_17)
- Chu G, Zhang ZY, Zhou H, Yan CX, Chen T, Guo YC. Research progress of age estimation based on age-related changes of Dentin-pulp complex. *Fa Yi Xue Za Zhi* 2018; **34**: 280–85. <https://doi.org/10.12116/j.issn.1004-5619.2018.03.013>
- Panchbhai AS. Dental radiographic indicators, a key to age estimation. *Dentomaxillofac Radiol* 2011; **40**: 199–212. <https://doi.org/10.1259/dmfr/19478385>
- Philippas GG. Influence of Occlusal wear and age on formation of Dentin and size of pulp Chamber. *J Dent Res* 1961; **40**: 1186–98. <https://doi.org/10.1177/00220345610400061301>
- Ikeda N, Umetsu K, Kashimura S, Suzuki T, Oumi M. Estimation of age from teeth with their soft X-Ray findings. *Nihon Hoigaku Zasshi* 1985; **39**: 244–50.
- Verma M, Verma N, Sharma R, Sharma A. Dental age estimation methods in adult Dentitions: an overview. *J Forensic Dent Sci* 2019; **11**: 57–63. [https://doi.org/10.4103/jfo.jfds\\_64\\_19](https://doi.org/10.4103/jfo.jfds_64_19)
- Karkhanis S, Mack P, Franklin D. Age estimation standards for a Western Australian population using the coronal pulp cavity index. *Forensic Sci Int* 2013; **231**: e1–6. <https://doi.org/10.1016/j.forsciint.2013.04.004>
- Koranne VV, Mhapuskar AA, Marathe SP, Joshi SA, Saddiwal RS, Nisa SU. Age estimation in Indian adults by the coronal pulp cavity index. *J Forensic Dent Sci* 2017; **9**(3): 177. [https://doi.org/10.4103/jfo.jfds\\_60\\_16](https://doi.org/10.4103/jfo.jfds_60_16)
- Drusini AG, Toso O, Ranzato C. The coronal pulp cavity index: a biomarker for age determination in human adults. *Am J Phys Anthropol* 1997; **103**: 353–63. [https://doi.org/10.1002/\(SICI\)1096-8644\(199707\)103:3<353::AID-AJPA5>3.0.CO;2-R](https://doi.org/10.1002/(SICI)1096-8644(199707)103:3<353::AID-AJPA5>3.0.CO;2-R)
- Havale R, Rao DG, Latha AM, Nagaraj M, Karobari NM, Tharay N. Coronal pulp: an age biomarker - A cross-sectional radiographic study in children. *J Oral Maxillofac Pathol* 2020; **24**: 389–94. [https://doi.org/10.4103/jomfp.JOMFP\\_342\\_19](https://doi.org/10.4103/jomfp.JOMFP_342_19)
- Andrade VM, Fontenele RC, de Souza AC, Almeida CA de, Vieira AC, Groppo FC, et al. Age and sex estimation based on pulp cavity volume using cone beam computed tomography: development and validation of formulas in a Brazilian sample. *Dentomaxillofac Radiol* 2019; **48**(7): 20190053. <https://doi.org/10.1259/dmfr.20190053>
- Kazmi S, Mânica S, Revie G, Shepherd S, Hector M. Age estimation using canine pulp volumes in adults: a CBCT image analysis. *Int J Legal Med* 2019; **133**: 1967–76. <https://doi.org/10.1007/s00414-019-02147-5>
- Yang F, Jacobs R, Willems G. Dental age estimation through volume matching of teeth Imaged by cone-beam CT. *Forensic Sci Int* 2006; **159 Suppl 1**: S78–83. <https://doi.org/10.1016/j.forsciint.2006.02.031>
- Cameriere R, Ferrante L, Cingolani M. Variations in pulp/tooth area ratio as an indicator of age: a preliminary study. *J Forensic Sci* 2004; **49**: 1–3. <https://doi.org/10.1520/JFS2003259>
- Ge Z, Ma R, Li G, Zhang J, Ma X. Age estimation based on pulp chamber volume of first molars from cone-beam computed tomography images. *Forensic Sci Int* 2015; **253**: 133. <https://doi.org/10.1016/j.forsciint.2015.05.004>
- Zheng Q, Ge Z, Du H, Li G. Age estimation based on 3D pulp Chamber Segmentation of first molars from cone-beam-computed tomography by integrated deep learning and level set. *Int J Legal Med* 2021; **135**: 365–73. <https://doi.org/10.1007/s00414-020-02459-x>
- Wang Y, Liu S, Wang G, Liu Y. Accurate tooth Segmentation with improved hybrid active contour model. *Phys Med Biol* 2018; **64**: 015012. <https://doi.org/10.1088/1361-6560/aaf441>
- Chung M, Lee M, Hong J, Park S, Lee J, Lee J, et al. Pose-aware instance Segmentation framework from cone beam CT images for tooth Segmentation. *Comput Biol Med* 2020; **120**: 103720. <https://doi.org/10.1016/j.combiomed.2020.103720>
- Thurzo A, Kosnáčová HS, Kurilová V, Kosmel' S, Beňuš R, Moravský N, et al. Use of advanced artificial intelligence in Forensic medicine, Forensic anthropology and clinical anatomy. *Healthcare (Basel)* 2021; **9**(11): 1545. <https://doi.org/10.3390/healthcare9111545>
- Lahoud P, EzEldeen M, Beznik T, Willems H, Leite A, Van Gerven A, et al. Artificial intelligence for fast and accurate 3-dimensional tooth Segmentation on cone-beam computed tomography. *J Endod* 2021; **47**: 827–35. <https://doi.org/10.1016/j.joen.2020.12.020>
- Yang Y, Xie R, Jia W, Chen Z, Yang Y, Xie L, et al. Accurate and automatic tooth image Segmentation model with deep Convolutional neural networks and level set method. *Neurocomputing* 2021; **419**: 108–25. <https://doi.org/10.1016/j.neucom.2020.07.110>
- Ronneberger O, Fischer P, Brox T. U-Net: Convolutional Networks for Biomedical Image Segmentation. Medical Image Computing and Computer-Assisted Intervention – MICCAI 2015. Lecture Notes in Computer Science 2015. p. 234–41.22.
- Nemoto T, Futakami N, Kunieda E, Yagi M, Takeda A, Akiba T, et al. Effects of sample size and data augmentation on U-Net-based automatic Segmentation of various organs. *Radiol Phys Technol* 2021; **14**: 318–27. <https://doi.org/10.1007/s12194-021-00630-6>
- Duan W, Chen Y, Zhang Q, Lin X, Yang X. Refined tooth and pulp Segmentation using U-Net in CBCT image. *Dentomaxillofac Radiol* 2021; **50**(6): 20200251. <https://doi.org/10.1259/dmfr.20200251>
- Zhang J, Xia W, Dong J, Tang Z, Zhao Q. Root Canal Segmentation in CBCT Images by 3D U-Net with Global and Local Combination Loss. In: Paper presented at the In: Paper presented at the 2021 43rd Annual International Conference of the IEEE Engineering in Medicine & Biology Society (EMBC), Mexico. <https://doi.org/10.1109/EMBC46164.2021.9629727>
- Smith BG, Knight JK. An index for measuring the wear of teeth. *Br Dent J* 1984; **156**: 435–38. <https://doi.org/10.1038/sj.bdj.4805394>
- Chen LP, Zhang DH, Que ZN. The investigation of tooth wear in 1033 adult patients. *J Clin Stomatol* 2007; **23**: 170–72.
- Tonetti MS, Greenwell H, Kornman KS. Staging and grading of Periodontitis: framework and proposal of a new classification and case definition. *J Clin Periodontol* 2018; **45**: S149–61. <https://doi.org/10.1111/jcpe.12945>
- Yang HF, Wang XW, Li G. Tooth and pulp Chamber automatic Segmentation with Artificial intelligence network and Morphometry method in cone-beam CT. *Int J Morphol* 2022; **40**: 407–13. <https://doi.org/10.4067/S0717-9502202000200407>
- Koo TK, Li MY. A guideline of selecting and reporting Intraclass correlation coefficients for reliability research. *J Chiropr Med* 2016; **15**: 155–63. <https://doi.org/10.1016/j.jcm.2016.02.012>
- Liu R, Du H, Li G. Prevalence and root curvature of Distolingual roots in Mandibular first molars in Beijing area population: three-dimensional analysis using cone-beam computed tomography images. *Beijing Journal of Stomatology* 2015; **30**: 111–14.
- Yu G, Ye L, Huang D. Clinical investigation of RADIX Entomolars in Mandibular first molars. *Hua Xi Kou Qiang Yi Xue Za Zhi* 2012; **30**: 259–61.
- Haghanifar S, Ghobadi F, Vahdani N, Bijani A. Age estimation by pulp/tooth area ratio in anterior teeth using cone-beam computed tomography: comparison of four teeth. *J Appl Oral Sci* 2019; **27**: e20180722. <https://doi.org/10.1590/1678-7757-2018-0722>
- Asif MK, Nambiar P, Mani SA, Ibrahim NB, Khan IM, Lokman NB. Dental age estimation in Malaysian adults based



- on volumetric analysis of pulp/tooth ratio using CBCT data. *Leg Med (Tokyo)* 2019; **36**: 50–58. <https://doi.org/10.1016/j.legalmed.2018.10.005>
37. Ge ZP, Yang P, Li G, Zhang JZ, Ma XC. Age estimation based on pulp cavity/chamber volume of 13 types of tooth from cone beam computed tomography images. *Int J Legal Med* 2016; **130**: 1159–67. <https://doi.org/10.1007/s00414-016-1384-6>
  38. Barbosa MG, Franco A, de Oliveira RDB, Mamani MP, Junqueira JLC, Soares MQS. Pulp volume Quantification methods in cone-beam computed tomography for age estimation: A critical review and meta-analysis. *J Forensic Sci* 2023; **68**: 743–56. <https://doi.org/10.1111/1556-4029.15248>
  39. Helmy MA, Osama M, Elhindawy MM, Mowafey B. Volume analysis of second molar pulp Chamber using cone beam computed tomography for age estimation in Egyptian adults. *J Forensic Odontostomatol* 2020; **38**: 25–34.
  40. Star H, Thevissen P, Jacobs R, Fieuws S, Solheim T, Willems G. Human dental age estimation by calculation of pulp-tooth volume ratios yielded on clinically acquired cone beam computed tomography images of Monoradicular teeth. *J Forensic Sci* 2011; **56** **Suppl 1**: S77–82. <https://doi.org/10.1111/j.1556-4029.2010.01633.x>
  41. Yeung M, Rundo L, Nan Y, Sala E, Schönlieb CB, Yang G. Calibrating the dice loss to handle neural network overconfidence for biomedical image Segmentation. *J Digit Imaging* 2023; **36**: 739–52. <https://doi.org/10.1007/s10278-022-00735-3>
  42. Dan Y, Zhu Z, Jin W, Li Z. S-Swin transformer: simplified Swin transformer model for Offline handwritten Chinese character recognition. *PeerJ Comput Sci* 2022; **8**: e1093. <https://doi.org/10.7717/peerj-cs.1093>
  43. Chen LC, Papandreou G, Kokkinos I, Murphy K, Yuille AL. Deeplab: semantic image Segmentation with deep Convolutional nets, Atrous Convolution, and fully connected Crfs. *IEEE Trans Pattern Anal Mach Intell* 2018; **40**: 834–48. <https://doi.org/10.1109/TPAMI.2017.2699184>